Journal of Environmental Management 240: 136-148 (2019)

Fingerprinting changes in source contribution for evaluating soil response during an exceptional rainfall in Spanish Pre-Pyrenees

Leticia Gaspar[1], Ivan Lizaga[1], William H. Blake[2], Borja Latorre[1], Laura Quijano[3], Ana Navas[1]

[1] Estación Experimental de Aula Dei, EEAD-CSIC, Avda. Montañana 1005, 50059 Zaragoza, Spain.

[2] School of Geography, Earth and Environmental Sciences, University of Plymouth, Plymouth, UK.

[3] Georges Lemaître Centre for Earth and Climate Research - Earth and Life Institute, Université Catholique de Louvain, Louvain-la-Neuve, Belgium.

* Corresponding author: *leticia.gaspar.ferrer@gmail.com*

Graphical Abstract

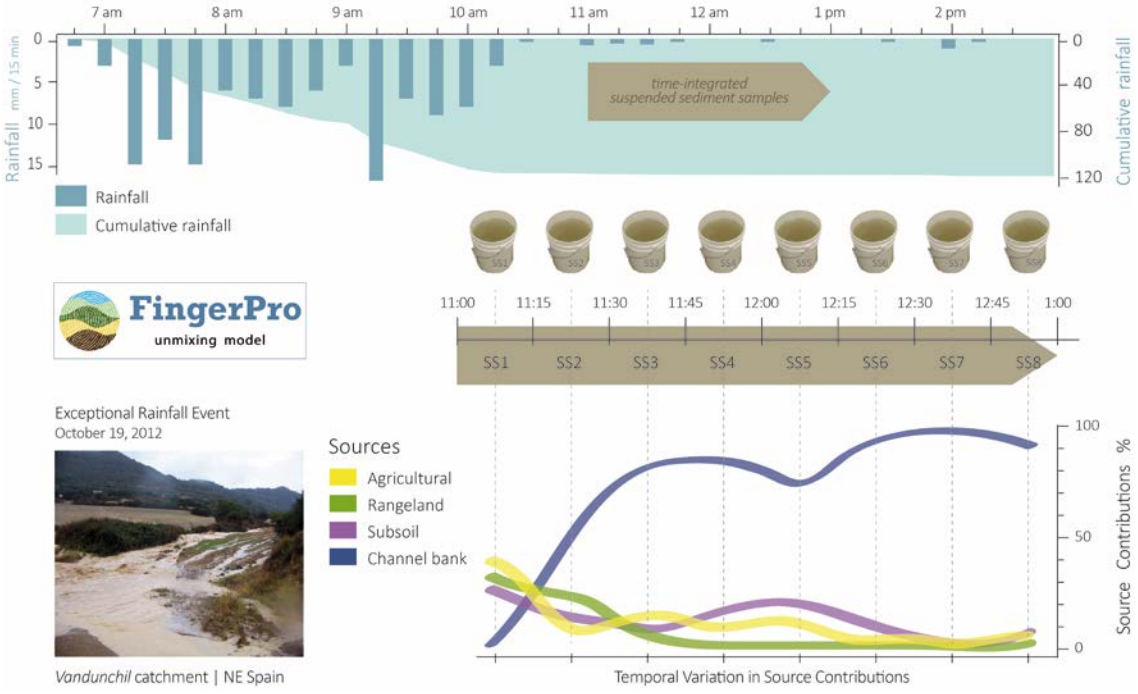

Highlights

- Unique opportunity to capture soil response during an exceptional event of 235 mm
- Suspended sediment properties changed during the flood event

- Source contributions varied in response to the rainstorm in a short period
- Switch from soil sources to channel bank provenance was captured during the flood
- Land use and connectivity determined the suspended sediment provenance

Abstract

In the Mediterranean region, floods are expected to increase as a result of climate change and knowledge of soil erosion hot spots during exceptional rainfalls is required to support mitigation measures. This study quantifies the main sediment sources during an exceptional rainfall event in 2012 (235 mm) at the outlet of two catchments located in NE Spain. To this purpose, suspended sediments were collected during the flood event, complemented with entrapped sediments in mat taken one year after the event. We used fingerprinting methodology and applied the FingerPro unmixing model to estimate the contribution from main sources. The selected tracers clearly distinguished agricultural, rangeland, subsoil and channel banks as the four potential sources in both catchments. In the *Vandunchil* catchment, the 8 time-integrated suspended sediment samples revealed changes in source contribution during the 2-hour sampling sequence. There were relatively high contributions from rangeland, agriculture and subsoil at the beginning of the sampling, representing 30, 40 and 35% of the total source contributions, respectively. Our records captured the delivery of pulses of eroded surface soil transported by runoff with direct connectivity to the stream. The sequence was followed by a sharp increase in channel bank contribution (up to 90%) in comparison to the other sources, reflecting streambank erosion and landslide occurrence, which manifested during the flood. In contrast, in the *La Reina* catchment, agricultural soils contributed the most (65%) and, together with subsoils (32%), were the main sources. These results reflect the effect of the higher connectivity and slope

gradient of these cultivated fields of the *La Reina* catchment in comparison with those of the *Vandunchil* catchment.

We discuss the possibility of using different properties, such as radionuclides, geochemistry and magnetic measurements, as tracers to distinguish between potential sources during an exceptional event in upland Mediterranean catchments. Our results support the use of fingerprinting techniques to determine variations in source contribution and sediment provenance during flood events, as extreme rainfalls are main drivers of sediment mobilization and key factors in changing landscapes. This is essential in identifying vulnerable hot spots, in which early-stage interventions are needed, and for helping policy makers with management of soil and water resources.

Keywords: Flood event; source provenance; suspended sediments; FingerPro model

1. Introduction

Exceptional rainfall events trigger large floods that result in severe soil and nutrient losses, important geomorphological changes. In general, during exceptional and extreme rainfall events with recurrence intervals of approximately 100 and more than 500 years, respectively, entire catchments are activated and extreme soil erosion and shallow landslides occur (Gonzalez-Hidalgo et al., 2013). The transport of enormous amounts of sediment produces severe soil and nutrient losses in some areas and sediment accumulation in others. The hydrological response of a catchment is related to the individual rainfall event and the characteristics of the catchment, such as water storage in the soil, antecedent soil moisture, land use, vegetation cover, topography and manmade infrastructures (Latron et al., 2008).

Erosion largely depends on a variety of factors, such as land use type, terrain, vegetation cover and type, inherent soil erodibility and intensity of erosive forces (e.g. Navas et al., 2008). Therefore, to control soil erosion, it is important to identify the most vulnerable areas that correspond with potential sources of mobilised sediments. Fine material in suspension is the major transport mechanism of particulate material in streams worldwide, typically comprising more than 90% of the annual load in alluvial streams (Meade et al., 1990). Lana-Renault et al. (2007) highlighted the importance of considering the changing locations of contributing areas of sediment during long-lasting rainstorms for understanding the complex hydrological and geomorphological behaviour of catchments. In Mediterranean environments, several studies have demonstrated that soils and vegetation cover are major factors explaining hydrological and sedimentological response caused by rainfall for different temporal and spatial scales (García-Ruiz, 2010).

Knowledge of sediment provenance is a key factor in understanding sediment transport and delivery processes (Walling, 2005). The fingerprinting technique has been successfully used to identify sediment sources in different physiographical regions around the world (Blake et al., 2012; Walling, 2013; Owens et al., 2016). The method assumes that the relative importance of potential sources can be determined by comparing several fingerprints in suspended sediment with those in potential sources. To document the suspended sediment provenance, tracer property values for the various potential sources are used in a mass balance equation to determine their relative contribution to the mixed signature in a suspended sediment sample (Collins and Walling, 2004). Different types of tracers have been used in published research including geochemistry (Laceby et al., 2015; Gaspar et al., 2019), radionuclides (Wallbrink et al., 1998; Collins and Walling, 2002; Gellis et al., 2017), colour

92 (Martínez-Carreras et al., 2010a; Pulley and Rowntree 2016; Barthod et al., 2015),
93 mineral magnetism (Oldfield and Wu, 2000; Rowntree et al., 2017), stable isotopes
94 (Revel-Rolland et al., 2005) and biomarkers (Hancock and Revill, 2013).

95 Research on sediment characteristics, including their sources and yields, can clarify
96 the physical and chemical properties of eroded soil, the potential nutrients and
97 pollutants associated, the transport and redistribution mechanisms and relationships
98 among sediment sources, sinks and outputs in rivers (Walling, 2005; Gellis and
99 Mukundan, 2013). The use of the fingerprinting technique for tracing soil and sediment
100 source response during rainstorms has received less attention compared with previous
101 studies documenting deposited flood sediments (Walling, 2013), partly due to the large
102 volumes of sample required to obtain sufficient sediment for tracing in a single, high-
103 rosivity flood event. Several studies have examined the potential for sediment
104 fingerprinting for recording single-erosion events using time-integrated samplers
105 (Martínez-Mena et al., 2010b; Cooper et al., 2014; Gellis et al., 2017; Rose et al., 2018).
106 However, although a number of studies have successfully applied various tracers to
107 discriminate potential source materials and investigated the temporal variations of
108 suspended sediment properties during rainfall events (Walling and Webb, 1982;
109 Horowitz et al., 2008), not many studies have captured temporal variation in sediment
110 sources in an effective way.

111 In this study, we aim to identify the temporal dynamics of sediment sources by
112 unmixing suspended sediments collected during an exceptional rainfall event that
113 occurred in 2012 in two adjacent mountain catchments in Northern Spain. Our main
114 purposes are: i) to describe the temporal variations of suspended sediment properties
115 during the time-integrated sampling, ii) to determine the contributions of the potential
116 sources for the suspended sediments and capture any temporal variations, and iii) to

117 compare the response of sediment sources to the exceptional rainfall event with records
118 occurring during more typical events by using sediment entrapped in mats samples.
119
120 **2. Study area**
121 The study was undertaken in two adjacent catchments located in the northern part
122 of the Ebro River Basin, Spain (Fig 1): *Vandunchil* catchment (15.3 km^2) and *La Reina*
123 catchment (1.8 km^2). The difference between the catchments lies largely in land use
124 distribution, slope gradients and hydrological connectivity.
125 The mean annual precipitation for the study area is around 500 mm (Quijano et al.,
126 2016). The hydrological regime is characterised by ephemeral streams and no
127 permanent rivers. Regular stream floods result from storms in late summer and autumn,
128 together with spring rains. The study catchments are ungauged and discharge data are
129 not available. Geomorphological features are conditioned by sub-horizontal
130 stratification of the lithostratigraphic units of the Uncastillo Formation.
131 The land use is primarily rangeland and agriculture land. Winter barley (e.g.
132 *Hordeum vulgare*) is the main crop in the cultivated areas. Rangeland is mostly
133 represented by scrubland, including patches of natural Mediterranean forest (e.g.
134 *Quercus coccifera* L.) and pine afforestation areas (e.g. *Pinus halepensis* Mill.) that are
135 restricted to the upper parts of the catchments.
136 The agricultural intensification increased connectivity due to enhanced overland
137 flow favouring gullying, stream incision, formation of channel banks and severe soil
138 erosion processes (Lizaga et al., 2019). On the other hand, the subsequent land
139 abandonment of some areas, in addition to the natural revegetation and pine
140 afforestation over the steep slopes during the past century, have significantly affected

141 the runoff response, reducing the connectivity and water erosion of these areas (Ligaza
142 et al., 2018).

143 The *Vandunchil* catchment has 82% of its surface area (12.6 km^2) occupied by
144 rangeland and 15% (2.3 km^2) by agriculture fields located in alluvial valley floors with
145 gentle slopes. Rangeland occupies steep-slope areas at the headwaters, with an
146 abundance of pine afforestation on terraces at the highest altitudes. The *La Reina*
147 catchment is occupied by nearly 40% (0.8 km^2) agriculture lands developed on
148 Quaternary steep glacis, while rangeland (1 km^2) occupies intermediate altitudes with
149 less terracing. Geomorphic features related to enhanced runoff (e.g. incised stream
150 banks) are less common in the *La Reina* catchment.

151

152 **3. Material and methods**

153 *3.1 The exceptional rainfall event*

154 In 2012, an exceptional rainfall, and subsequent flood, event occurred in the
155 central-western Pyrenees with rainfall totalling approximately 235 mm in a two-day
156 period, from October 19-21, 2012. The event was recorded using a tipping bucket rain
157 gauge. The precipitation at the study site coincides with that measured at the Yesa
158 weather station (WS) (217.2 mm, with measurements taken every 15 minutes) located
159 20-km north of the study site.

160 The event began at 6:45 am. A total of 121 mm of rain accumulated in less than 5
161 hours, with a peak intensity of 17 mm/15 min at 9:15 am, two hours before the sampling
162 started. Stream response time, based on local observations of flooding, was estimated at
163 1-2 hours after storms (resident personal communication). Figure 2 shows the
164 hydrograph for Yesa WS during the event. No human lives were lost, although the

floods destroyed roads, enlarged some parts of the alluvial plain and caused landslides in the channel banks (Fig. 3).

3.2 Sampling collection

Potential source materials were sampled across the two catchments. After several field inspections, four primary sediment sources were identified: (1) agricultural topsoil, (2) rangeland topsoil, (3) bare subsoil surfaces exposed to erosion, and (4) channel banks. The number of samples obtained was approximately proportional to the area occupied by each source type (Fig. 1). Surface soils were sampled using cylindrical cores 5 cm long and 6 cm in diameter. Three samples were obtained at each site to create composite samples that were combined in the field. For the *Vandunchil* catchment, a total of 106 source samples were collected as follows: agricultural (11), rangeland (78), subsoil (7) and channel banks (10), respectively. For the *La Reina* catchment, a total of 43 source samples were obtained: agricultural (20), rangeland (14), subsoil (6) and channel banks (3).

The set of downstream sediment mixtures comprised 10 suspended sediment (SS) samples collected during the flood event, and another four sediment samples entrapped in mats (SM) collected in 2013, one year after the event. The suspended sediment samples were collected in *situ* at the outlet of both ungauged catchments (see Fig 2). A total of 10 grab samples of stream water were collected periodically during the flood. Eight 5-L bucket samples were taken every 15 minutes during a 2-hour period at the outlet of the *Vandunchil* catchment, and two buckets were taken at the outlet of the *La Reina* catchment. In November 2012, after the storm event, 4 sediment trap sites were installed for the two catchments: three in the *Vandunchil* catchment and one at the outlet of the *La Reina* catchment (Fig. 1). Each individual trap site consisted of three pieces of

190 artificial turf (25 x 40 cm^2) secured to the surface with 10-cm long steel pins. A total of
191 12 sediment mat traps were in place for nearly one year, during which no additional
192 exceptional events occurred.
193
194 *3.3 Lab analyses*
195 The sediment source, SS and SSC samples were air-dried, gently disaggregated,
196 and sieved to <63 μm. The suspended sediments (SS) were obtained by decanting the
197 water contained in the 5-L buckets, and the suspended sediment concentration (SSC)
198 was measured after filtering the water samples and drying the residue. Sediments
199 entrapped in mats (SM) were extracted from the artificial turf.
200 Gamma emissions of ^{137}Cs, ^{226}Ra, ^{238}U, ^{232}Th, and ^{40}K were measured using a
201 Canberra Xtra high-resolution, low-background, hyperpure germanium coaxial gamma
202 detector (50% efficiency, 1.9-keV resolution) (Navas et al., 2013). Count times over a
203 24-hr period provided an analytical precision of about ±3-10% at a 95% level of
204 confidence. The radionuclide activities are expressed as Bq kg^{-1} dry soil.
205 Elemental geochemistry was analysed by X-ray fluorescence (XRF) using a
206 Thermo Fisher Scientific Niton XL3T 950 He GOLDD XRF analyser. Samples were
207 packed into XRF sample cups with a 38.2-mm exposure diameter which permits the X-
208 Ray pulse (3-mm diameter) to strike the surface of the sample. Helium was used to
209 allow measurement of light elements, resulting in 18 elements with measurements
210 above the detection limit (Ba, Nb, Zr, Sr, Rb, Pb, Zn, Fe, Cr, V, Ti, Ca, K, Al, P, Si, S,
211 and Mg). Analytical quality controls recorded a very low drift of less than 1%. The
212 mass concentration is expressed as ppm.
213 Low-frequency magnetic susceptibility (LF) was determined using a Bartington
214 susceptibility meter. The content of soil organic carbon (SOC) was measured by using a

dry-combustion method LECO RC-612 multiphase carbon analyser (LECO Corporation, St. Joseph, MI, USA). Particle size analyses were performed using a Coulter LS 13 320 laser diffraction particle size analyser (Beckman Coulter, Inc., 2011), after eliminating the organic matter.

3.4 Fingerprinting procedure

Standard statistical tests were used for selecting the optimal tracers (Palazón et al., 2015, Gaspar et al., 2019). The FingerPro unmixing model (Lizaga et al., 2018a) was used for estimating the contributions of sediment sources in the SS and SM samples. A total of 42 simulations were performed, evaluating three different sets of tracers: i) including P, ii) excluding P, and iii) including SOC and P.

FingerPro is a standard linear multivariate unmixing model with Monte Carlo uncertainty analysis implemented in an open-source R package within the CRAN platform (Lizaga et al., 2018a). The relative contribution of each sediment source is determined following equation 1, which satisfies the constraints of equation 2:

$$\sum_{j=1}^{m} a_{i,j} \cdot \omega_j = b_i$$

$$\sum_{j=1}^{m} \omega_j = 1 \qquad 0 \leq \omega_j \leq 1,$$

where b_i is the tracer property i (i =1 to n) of the sediment mixture, $a_{i,j}$ represents the tracer property i in the source type j (j =1 to m), ω_j is the unknown relative contribution of the source type j, m represents the number of potential sediment sources and n is the number of tracer properties selected. The procedure aims to find the source proportions that conserve the mass balance, where apportionments must lie between 0 and 1 and sum 1, expressed in % (i.e. between 0 and 100, sum of 100). The source contributions estimated by the FingerPro model were expressed as the mean source contribution (pie-

239 chart) and the frequency distribution (violin plot) of the best 100 solutions predicted by
240 the model.
241
242 **4. Results**
243 *4.1 Characteristics of the sediment sources and mixtures*
244 The most abundant element in the sediment sources was Si, with a maximum
245 content of 251,272 ppm. Other major elements were Ca, Al, Fe, and K (9,037-251,272
246 ppm), followed by Mg, P, Ti, Sr and Mn (109-7,528 ppm). Contents of Ba, Zr, Rb, Zn,
247 Cr, and V ranged from 30 to 559 ppm and the trace elements Pb and Nb were below 33
248 ppm. The LF value ranged from 5 to 146 10^{-8} m^3 kg^{-1}, and SOC content varied from
249 undetectable to 7%. The mass activity of ^{137}Cs ranged from 0 to 33 Bq kg^{-1}, the mean
250 activity of ^{40}K reached 500 Bq kg^{-1}, while the mean activities of ^{226}Ra, ^{232}Th and ^{238}U
251 were lower than 50 Bq kg^{-1}, falling within ranges of similar soils (Navas et al., 2005).
252 Most sediment source properties had similar ranges in both catchments, although
253 the mean values of ^{137}Cs, LF and SOC were nearly twice in *Vandunchil* catchment than
254 in *La Reina* catchment. For the sediment mixtures, most suspended sediment properties
255 fell within the 5^{th}-95^{th} percentile range of values found in the source groups. However,
256 sediments entrapped in mats had a larger number of properties with values outside the
257 sediment source ranges (e.g. Al, Fe, Rb, Zn, Mn, or ^{40}K) (Table 1).
258 During the time-integrated sampling sequence (SS1 to SS8) at the outlet of
259 *Vandunchil* catchment, activities of ^{137}Cs, ^{40}K, ^{238}U, ^{226}Ra, ^{232}Th and LF values
260 decreased, with the exception of a sharp increase in SS3 related to an increase in
261 contents of Ca, Se, Zr, P and sand fraction (Fig. 4). There was also a clear decreasing
262 trend in SOC, Al, Fe K, Mg, Rb, Zn, V, and clay content. In contrast, Si, Ca, Sr, P, Zr,
263 and sand content increased, while Ti, Nb, and Pb varied little. The suspended sediment

264 concentration was lower at the beginning of the sampling sequence (7.3 gL^{-1} in SS1)
265 and progressively increased to concentrations up to 26.5 gL^{-1} in SS8 (Fig. 4).

266 In *La Reina* catchment, there were no differences in most properties apart from a
267 slight increase in Mg, Se, and Ca, and a slight decrease in Ba, Mn, and Nb contents. The
268 SSC was 19.3 and 17.9 gL^{-1} in SS1' and SS2', respectively.

269

270 *4.2 Source discrimination and tracer selection*

271 Almost 75% and 50% of the sediment source properties were significantly different
272 between the four source groups at the *Vandunchil* and *La Reina* catchment, respectively
273 (Table 1). In the *Vandunchil* catchment, agricultural soils had significantly higher mean
274 contents of P and clay fraction than the other sources. Rangeland soils were
275 characterised by the highest means of ^{137}Cs, SOC, Si, Fe, Cr and Pb, but had
276 significantly lower contents of Ca, Sr, and Ba than in subsoils. Subsoils recorded the
277 highest contents of Ca, K, Mg, Sr, Ba, Rb, and V, and the lowest of P, SOC, Mn, and Zr
278 contents. Channel banks had significantly lower mean of Fe, Ti, Cr, Zn, and clay
279 contents than the other sources. Like subsoil and agricultural soils, channel banks had
280 also low SOC and high Zr contents. Similarly to subsoils, channel banks had low LF
281 and ^{137}Cs activity (Table 1).

282 In *La Reina* catchment, agricultural soils had significantly higher mean P and ^{226}Ra
283 contents than the other sources, while the highest ^{137}Cs and SOC were in rangeland
284 soils. Subsoils registered significantly higher means of Mg, Sr, and sand content but
285 lower mean of SOC, P, LF, and Ti than the other sources. Channel banks were enriched
286 in Ti and Zr, similar to rangeland soils, and in Ba similar to subsoils. However, mean Cr
287 content was significantly lower than in the other sources (Table 1).

Different properties, in number and type, were selected as optimum composite fingerprint tracers (Table 2). For the *Vandunchil* catchment, the first seven suspended sediment samples (SS1 to SS7) had the same 9 optimum fingerprints. In most cases, ^{137}Cs and LF were the selected tracers, followed by Fe (except for SS8 and SM), Ba and Cr (except for SM1), P (except for SM2), and Ca (except for SM3). Tracers like Ti and V were also selected for most sediment mixtures except for SM1 and SM3. For the *La Reina* catchment, fewer properties met the selection criteria, but similar to the *Vandunchil* catchment, ^{137}Cs, Ba, Ti, and P were the selected tracers, along with Mg. In addition, tracers like Zr and Sr were used for SS1' and SS2'.

Both catchments showed a clear discrimination between the four sources (Fig. 5). Discriminant function analysis (DFA) plots show a clear distinction between subsoils and channel banks. Differences were less clear between agricultural and rangeland soils because overlapping occurred for some samples, especially in the *Vandunchil* catchment. Despite that, for both catchments, DFA step-wise produced a set of tracers that allowed correct classification of 100% of the channel bank samples, 98% of subsoils and around 90% of agricultural and rangeland soils.

4.3 Source contributions for the suspended sediments

In the *Vandunchil* catchment, the source provenance for the time-integrated sampling varied greatly from SS1 to SS3, with little variations observed from SS4 to SS8. The contribution from agricultural and rangeland soils decreased exponentially during the sampling sequence. A similar decreasing pattern, but less evident, occurred for the subsoil contributions (Fig. 6). However, apportions from channel bank had a clear exponential increase from SS1 to SS8.

312 The dispersion of the source contributions varied from low SD values (0.7 %) up to
313 19% (Table 3). Agricultural and rangeland soils yielded the highest SDs in SS1 to SS3,
314 but the lowest in SS4 to SS8. The SDs for subsoil were consistently around 7%, while
315 channel bank saw a low SD in SS1 and high SDs in SS2 to SS8. These results changed
316 when P was excluded as an optimum tracer, resulting in increased uncertainty for all
317 sources. Inclusion of SOC did not affect uncertainty estimates (Table 3).

318 The frequency distributions of the estimated subsoil contributions showed narrow,
319 symmetrical and unimodal distributions. Agricultural and rangeland contributions for
320 SS1 showed symmetrical frequency distributions, while for SS6 to SS8 the symmetrical
321 distributions where less clear. A multimodal pattern was observed in SS3 for the
322 agricultural soils (Fig 6).

323 In the *La Reina* catchment, similar source contributions were estimated for SS1'
324 and SS2'. The agricultural soils contributed the most, more than doubling the subsoils
325 apportions. The rangeland soils and channel bank together, contributed less than 2% and
326 7% for SS1' and SS2', respectively. The range of solutions varied little (SD from 1.7 to
327 9%), especially for SS1' with SD values lower than 6.5%. The frequency distribution
328 for agricultural soils and subsoil was symmetrical and unimodal, whereas for rangeland
329 soils and channel bank was less symmetric but narrow enough (Fig. 7).

330

331 *4.4 Source contributions for the sediment entrapped in mats*

332 Different source contributions, depending on the location of the mats, were
333 observed in the *Vandunchil* catchment. Sediment mat SM1, located upstream of SM2,
334 recorded channel bank as the main apportion. In contrast, SM2 showed that subsoil was
335 the main contributing source, with around 20% sourced from channel bank. The
336 dispersion of the results was higher in SM2 than in SM1, but with SD lower than 7% for

most estimated source contributions, apart from channel bank and subsoil in SM2 (Fig. 6). After several trials, it was not possible to unmix SM3.

At the outlet of the *La Reina* catchment, SM1' showed similar source contributions to the suspended sediment samples SS1' and SS2' (Fig. 7). Agricultural soil was the predominant source and contributed almost three times more than subsoil. However, the contribution of rangeland soils and channel bank in SM1' was at least twice as much as the contribution recorded for SS1' and SS2' (Table 4). Despite similarities between the results obtained for suspended sediments and the sediment entrapped in mats, SM1' had wider and less symmetric frequency distributions than those of the suspended sediments samples (Fig. 7).

5. Discussion

5.1 Optimum composite fingerprints

The capability of ^{137}Cs in discriminating between sediment sources is a result of large differences between ^{137}Cs activities in the soil sources. The high ^{137}Cs mass activity in rangeland reflects the effect of vegetation cover's protection of the soil surface while the low content in agricultural soils is due to dilution by mixing during tillage (Gaspar et al., 2013). For the other sources, the absence of the radionuclide is consistent with erosion of topsoil layers in subsoil, while verticality of channel banks prevents ^{137}Cs tagging with the bank materials. Large contents of Sr, Ca, Ba, Mg, V, and K in subsoil are related to the carbonatic characteristics of parent materials, which concentrate these elements (Navas and Machín, 2002), but also to the high capacity of clay minerals to absorb these elements (Kabata-Pendias and Pendias, 2001; Navas and Lindhorfer, 2003). The low Ti content in subsoil might reflect the effects of weathering. As Ti minerals are very stable, the loss of some clay-size layered silicates might

362 increase the amount of Ti in the upper soil horizons (Kabata-Pendias and Pendias,
363 2001). Therefore, the better-developed and undisturbed soils, such as in rangeland
364 sources, could be more enriched in Ti than eroded areas, represented by subsoil.

365 Differences in Fe between sources are likely related to oxides and hydroxides that
366 are more abundant in better-developed soils, which predominate in rangeland. The
367 highest SOC contents and LF values in rangeland are in agreement with significant
368 positive correlations between SOC and magnetic properties, also reported by Quijano et
369 al. (2014) and confirm the potential for using magnetic properties in tracking soil
370 degradation in this environment. Mineral magnetism was also successfully applied as a
371 single tracer for suspended sediments samples collected through consecutive storm
372 events in South Africa (Rowntree et al., 2017).

373 Though controversies about the use of nutrients as tracers persist, largely due to
374 their potentially non-conservative behaviour during transport (Withers and Jarvie, 2008;
375 Koiter et al., 2013), P is used to investigate the contribution of sediment related to
376 agricultural activities (Walling et al., 2008) and can track cropland or pasture erosion
377 (Ben Slimane et al., 2013; Lamba et al., 2015). We used P and SOC because of the short
378 transport length, the brief duration of the sampling sequence, and the rapid flood that
379 prevented soil storage (Blake et al., 2006).

380 Both P and SOC are of value for distinguishing between sources. The benefits of
381 including them as tracers relate to providing less variability to the source contributions
382 (Tables 3 and 4, see GOF values). The significantly higher content of P in agricultural
383 soils than in the other sources supports its likely origin from fertilisers. In addition,
384 alkaline soils in the study area, with low SOC and secondary accumulation of
385 carbonates, may play an important role in the equilibria between the particulate and

386 dissolved P fractions through the possible presence in our soils of the carbonate-
387 fluorapatite mineral (Ca_5 (PO_4, CO_3)) (OH, F)) (Vidal, 1988).

388 The high values of Ca, P, and sand content that peak in SS3, in coincidence with
389 low clay content, denote a common mineral origin. The increase of P and Ca from SS4
390 to SS8, in which we estimated a clear predominance of channel bank soil contribution
391 also supports a mineral origin for P. Further, the enriched Ca content in subsoil and
392 channel banks, in line with the presence of Ca in different forms, increases the soil
393 retention capacity of P, which binds readily to Ca. Other soil characteristics, like SOC,
394 pH, and texture, also influence the availability of P in soil (i.e. finer textures have a
395 greater capacity to replace P than coarser textures). Furthermore, sediment deposition in
396 channel beds, and subsequent remobilization, exert an important influence on the
397 transport and fate of particulate P in catchments (Owens and Walling, 2002). Jarvie et
398 al. (2005) observed that P stored in sediments can be re-released as dissolved P after
399 reduction, though such releases would make small changes to the overall P signature at
400 our scale. Further, soil erosion processes have also been shown to affect the partitioning
401 of P between dissolved vs. particulate forms during runoff events (Huisman et al., 2013)

402 Our results are in agreement with the developing idea that tracer selection should be
403 also supported by knowledge of hydrological, geomorphological, and geochemical
404 processes controlling tracer behaviour. Other studies also support the selection of
405 appropriate soil properties as fingerprinting tracers not solely on the basis of statistical
406 procedures (e.g., Smith et al., 2018).

407

408 *5.2 Source contribution variations during the flood event*

409 A varied response to the rainfall event and runoff was clearly detected between the
410 two adjacent study catchments, reflecting, among others, differences in land use,

411 physiography and connectivity in the catchments. To this respect, in the *La Reina*
412 catchment, agricultural soils are the major source of suspended sediments because of its
413 higher connectivity and steeper slopes of cultivated fields in contrast with the
414 *Vandunchil* catchment.

415 In the *Vandunchil* catchment at the beginning of the extreme flood, agricultural and
416 rangeland topsoils were primary sources, along with subsoil. However, as the event
417 progressesed, channel bank become the main source. The agricultural contribution in
418 the early stages of the flood is indicated by higher SOC content at the beginning of the
419 sampling sequence, rather than later. Although runoff transported rangeland soil
420 particles at the initiation of the event, its signal declined later. A reason could be the
421 topography of the catchment with clear sub-horizontal stratification, along with the
422 abundance of linear elements due to terracing for pine afforestation that retain the
423 mobilised sediments. In addition, vegetation cover seems efficient in protecting soil and
424 preventing further sediment mobilization, even under this exceptional disturbance.

425 In contrast, evidence of streambank erosion from SS4 to SS8 is supported by the
426 predominant contribution of channel bank and the highest SSC values. The importance
427 of streambank erosion is further evidenced by changes in the channel section observed
428 after the exceptional rainfall, which produced streambanks failure that resulted in a
429 widening of the channel section. Palmer et al. (2014) also recorded high streambank
430 erosion when precipitation was 26% above normal. Factors affecting bank erosion
431 under high flooding conditions are related to the hydraulic forces exerted on the stream,
432 which create unstable conditions that result in bank failure and mass wasting (Wynn,
433 2006).

434 The suspended sediment dynamic and the temporal variability of the relative source
435 contributions are linked to several factors, including the distribution of land uses,

436 connectivity, and changes in the stream channel (i.e. failure of loose streambanks) (Fig.
437 2). Other authors also point to sediment connectivity, in addition to modifications in
438 contributing areas (Evrard et al., 2010), hydraulic boundary and antecedent soil
439 moisture conditions.

440 This study has captured the signal of rangeland soils that, under regular rainfall, is
441 difficult to obtain because these soils are protected by vegetation cover and terracing.
442 The field observations during and after the storm event allowed us to identify intense
443 rilling and new gully formation in agricultural and rangeland soils that support the
444 estimated source apportions. Our results suggest that the new connectivity created
445 during the event worked efficiently to transport sediment to the stream. This indicates
446 that connectivity between the headwaters and our sampling locations was unobstructed
447 and was able to effectively transport sediments throughout the stream channel. In earlier
448 work, Koiter et al. (2013) similarly highlight the importance of the sampling location
449 and the need to incorporate the catchment connectivity to understand how efficiently the
450 sediment is transported from the headwaters to the outlet. In the *La Reina* catchment,
451 comparable results obtained for the suspended sediments (SS1', SS2') and for the
452 sediment mat (SM1') confirm that source contributions were similar during the
453 exceptional rainfall and during periods of regular precipitation. The high connectivity of
454 the catchment and the predominance of agricultural soils on Quaternary steep glacis is
455 the reason why these soils are the major source of sediments.

456 Under regular functioning of ephemeral streams, the main difference of an
457 exceptional event is that rangeland soils and, to lesser extent, agricultural soils and
458 subsoils are less well connected with the drainage system because of terracing,
459 vegetation strips, furrows, and other linear elements of the landscape that protect soil
460 from erosion (Lizaga et al., in press). Fryirs (2013) identified three types of blockages

461 (buffers, barriers, and blankets), indicating that their spatial arrangement will exert an
462 influence on the connectivity and, subsequently, on the pattern of sediment transport
463 and storage (Hooke and Mant, 2000; Kuo and Brierley, 2013). However, for intense
464 rainfalls, the connectivity of agricultural and rangelands increases, leading to high
465 sediment loads in the streams. Only unusual high-magnitude events like this event are
466 able to produce enough surface runoff to connect the hydrological system with the
467 sources of sediment. After soil particles are disaggregated by runoff, due to fluctuations
468 in runoff transport capacity, the particles can be temporarily stored inside the fields,
469 preventing them from reaching the streams. On the other hand, the large discharges that
470 reach the streams increase channel erosivity and cause landslides thus increasing the
471 signal of channel bank.

472 Our results during this exceptional event, along with previous research on
473 connectivity in the study area (Lizaga et al., 2019), allow us to better understand the
474 variation of source apportions. Due to human impact on Mediterranean landscapes,
475 these uplands agroecosystems streams produce infilling of valley floors that are later
476 incised. The landscape evolution has led to the presence of a mosaic of land uses and
477 different surface covers that influence the connectivity of sediment sources to the river
478 network. We can conclude that the change in dominant source during the sampling
479 sequence in the *Vandunchil* catchment is due to changes in sediment storage and
480 connectivity, reflecting a transition in the dominant erosion processes from topsoil to
481 streambank erosion.

482

483 **6. Conclusions**

484 This study provided a detailed record of temporal variations in relative source
485 contributions to the total sediment flux through time during an exceptional rainfall

event. Our results demonstrated the potential for using ^{137}Cs, along with stable elements and magnetic properties as effective tracers. In addition, our study has proven the efficiency of the FingerPro model in determining quantitative source contributions to capture a change in dominant source. The different characteristics of the study catchments, in terms of distribution of land uses and structural connectivity of the landscape, played a key role in controlling sediment availability and the prominence of the contributing source. The rainfall event activated the entire *Vandunchil* catchment, transporting sediment from sources that, during regular flood events, remain disconnected, and allowed for the sediment to surpass the linear elements that typically interrupt the connectivity of the landscape. The predominant contributions of agricultural, rangeland and subsoil sources, in addition to the lowest concentration of suspended sediments and the highest SOC contents support topsoil erosion occurring at the beginning of the exceptional event, while later peaks of SSC and high contributions of channel bank suggest a shift to predominance of streambank erosion.

One of the main findings from our study is the temporal variability in source provenance recorded during the 2-hour sampling sequence at the outlet of the *Vandunchil* catchment, which demonstrates the need to generate high spatial and temporal resolution source apportionments, especially during storm-events.

Sediment fingerprinting approaches offer important insights into the nature of erosion and transport processes that operate in Mediterranean upland catchments supporting that exceptional events are main drivers of the process dynamic leading to landscape changes.

Acknowledgements

This research was funded by the project (CGL2014-52986-R). We thanks Dr Javier Machín for the valued rainfall records and sampling data obtained during the exceptional rainfall event.

References

Barthod, L.R., Liu, K., Lobb, D.A., Owens, P.N., Martínez-Carreras, N., Koiter, A.J., Petticrew, E.L., McCullough, G.K., Liu, C., Gaspar, L., 2015. Selecting Color-based Tracers and Classifying Sediment Sources in the Assessment of Sediment Dynamics Using Sediment Source Fingerprinting. J Environ Qual. 44(5), 1605–16.

Blake, W.H., Walsh, R.P.D., Sayer, A.M., Bidin, K., 2006. Quantifying fine-sediment sources in primary and selectively logged rainforest catchments using geochemical tracers. Water, Air, and Soil Pollution: Focus 6(5–6), 615–623.

Blake, W.H., Ficken, K.J., Taylor, P., Russell, M.A., Walling, D.E., 2012. Tracing cropspecific sediment sources in agricultural catchments. Geomorphology 139–140, 322–329.

Ben Slimane, A., Raclot, D., Evrard, O., Sanaa, M., Lefèvre, I., Ahmadi, M., Tounsi, M., Rumpel, C., Ben Mammou, A., Le Bissonnais, Y., 2013. Fingerprinting sediment sources in the outlet reservoir of a hilly cultivated catchment in Tunisia. J. Soils Sediments 13, 801–815.

Collins, A.L., Walling, D.E., 2002. Selecting fingerprint properties for discriminating potential suspended sediment sources in river basins. J. Hydrol. 261, 218–244.

Collins, A.L., Walling, D.E., 2004. Documenting catchment suspended sediment sources: problems, approaches and prospects. Prog. Phys. Geogr. 28, 159–196.

536 Evrard, O., Nord, G., Cerdan, O., Souchère, V., Le Bissonnais, Y., Bonté, P., 2010.
537 Modelling the impact of land use change and rainfall seasonality on sediment export
538 from an agricultural catchment of the northwestern Environ. 138 (1–2), 83–94.
539 European loess belt. Agric. Ecosyst.

540 Fryirs, K., 2013. Disconnectivity in catchment sediment cascades, a fresh look at
541 the sediment delivery problem. Earth Surf. Process. Landf. 38, 30–46.

542 García-Ruiz, J.M.., 2010. The effects of land uses on soil erosion in Spain. A
543 review. Catena 81(1), 1–11.

544 Gaspar, L., Navas, A., 2013. Vertical and lateral distributions of ^{137}Cs in cultivated
545 and uncultivated soils on Mediterranean hillslopes. Geoderma 207–208, 131–143.

546 Gaspar, L., Navas, A.,Walling, D.E.,Machín, J., Gómez Arozamena, J., 2013.
547 Using ^{137}Cs and $^{210}Pb_{ex}$ to assess soil redistribution on slopes at different temporal
548 scales. Catena 102, 46–54.

549 Gaspar, L., Blake, W.H., Smith, H. G., Lizaga, I, Navas, A., 2019. Testing the
550 sensitivity of a multivariate mixing model using geochemical fingerprints with artificial
551 mixtures. Geoderma 337, 498–510.

552 Gellis, A.C., Mukundan, R., 2013. Watershed sediment source identification: tools,
553 approaches and case studies. J. Soils Sediments 13, 1655–1657.

554 Gellis, A.C., Fuller, C.C., Van Metre, P.C., 2017. Sources and ages of fine-grained
555 sediment to streams using fallout radionuclides in the Midwestern United States. J.
556 Environ. Manag. 194, 73–85.

557 Gonzalez-Hidalgo, J.C., Batalla, R.J., Cerda, A., 2013. Catchment size and
558 contribution of the largest daily events to suspended sediment load on a continental
559 scale. Catena 102, 40–45.

560 Hancock, G.J., Revill A.T., 2013. Erosion source discrimination in a rural
561 Australian catchment using compound-specific isotope analysis (CSIA). Hydrol Process
562 27:923–932.
563 Hooke, J.M., Mant, J.M., 2000. Geomorphological impacts of a flood event on
564 ephemeral channels in SE Spain. Geomorphology 34, 163–180.
565 Horowitz, A.J., 2008. Determining annual suspended sediment and sediment-
566 associated trace element and nutrient fluxes. Sci. Total Environ. 400 (1–3), 315–343.
567 Huisman, N.L.H., Karthikeyan, K.G., Lamba, J., Thompson, A.M., Peaslee, G.,
568 2013. Quantification of seasonal sediment and phosphorus transport dynamics in an
569 agricultural watershed using radiometric fingerprinting techniques. J. Soils Sediments
570 13 (10), 1724–1734.
571 Jarvie, H.P., Jürgens, M.D., Williams, R.J., Neal, C., Davies, J.J.L., Barrett, C.,
572 White, J., 2005. Role of river bed sediments as sources and sinks of phosphorus across
573 two major eutrophic UK river basins: the Hampshire Avon and Herefordshire Wye. J.
574 Hydrol. 304 (1), 51–74.
575 Kabata-Pendias, A., Pendias, H., 2001. Trace Elements in Soils and Plants. CRC,
576 Boca Raton, p. 315.
577 Koiter, A.J., Owens, P.N., Petticrew, E.L., Lobb, D.A., 2013. The behavioural
578 characteristics of sediment properties and their implications for sediment fingerprinting
579 as an approach for identifying sediment sources in river basins. Earth Sci. Rev. 125, 24–
580 42.
581 Kuo, C.W., Brierley, G.J., 2013. The influence of landscape configuration upon
582 patterns of sediment storage in a highly connected river system. Geomorphology 180–
583 181, 255–266.

584 Laceby, J.P., Olley, J., 2015. An examination of geochemical modelling approaches
585 to tracing sediment sources incorporating distribution mixing and elemental
586 correlations. Hydrol. Process. 29 (6), 1669–1685.
587 Lamba, J., Karthikeyan, K.G., Thompson, A.M., 2015b. Using radiometric
588 fingerprinting and phosphorus to elucidate sediment transport dynamics in an
589 agricultural watershed. Hydrol. Process. 29, 2681–2693.
590 Lana-Renault, N., Regues, D., Marti-Bono, C., Begueria, S., Latron, J., Nadal, E.,
591 et al., 2007. Temporal variability in the relationships between precipitation, discharge
592 and suspended sediment concentration in a small Mediterranean mountain catchment.
593 Nord. Hydrol. 38, 139–150.
594 Latron, J., Soler, M., Llorens, P., Gallart, F., 2008. Spatial and temporal variability
595 of the hydrological response in a small Mediterranean research catchment (Vallcebre,
596 Eastern Pyrenees). Hydrological Processes 22, 775–787.
597 Lizaga I., Latorre B., Gaspar L., Navas A., 2018. fingerPro: An R package for
598 sediment source tracing, https://doi.org/10.5281/zenodo.1402029.
599 Lizaga, I., Quijano, L., Palazón, L., Gaspar, L., Navas, A., 2018. Enhancing
600 connectivity index to assess the effects of land use changes in a Mediterranean
601 catchment. Land Degrad. Develop. 29: 663–675.
602 Lizaga, I., Quijano, L., Gaspar, L., Ramos, M.C., Navas, A., 2019. Linking land use
603 changes to variation in soil properties in a Mediterranean mountain agroecosystem.
604 Catena 172, 516–527.
605 Lizaga, I., Gaspar, L., Latorre, B., Blake, W.H., Navas, A. Fingerprinting changes
606 of Sources apportionments and soil properties variation pre- and post- exceptional
607 rainstorm event. Geomorphology, *in press*.

608 Martínez-Carreras, N., Udelhoven, T., Krein, A., Gallart, F., Iffly, J.F., Ziebel, J.,
609 Hoffmann, L., Pfister, L., Walling, D.E., 2010a. The use of sediment colour measured
610 by diffuse reflectance spectrometry to determine sediment sources: application to the
611 Attert River catchment (Luxembourg). J. Hydrol. 382, 49–63.
612 Martínez-Carreras, N. F., A. Krein, T. Udelhoven, F. Gallart, J. F. Iffly, L.
613 Hoffmann, L. Pfister, and D. E. Walling., 2010b. A rapid spectral-reflectance-based
614 fingerprinting approach for documenting suspended sediment sources during storm
615 runoff events, J. Soils Sediments, 10(3), 400–413.
616 Meade, R.H., Yuzyk, T.R., Day, T.J., 1990. Movement and storage of sediment in
617 rivers of the United States and Canada. The Geology of North America, Vol 0–1,
618 Surface Water Hydrology. The Geological Society of America, pp. 225–280.
619 Navas, A., Machín, J., 2002. Spatial distribution of heavy metals and arsenic in
620 soils of Aragon (northeast Spain): controlling factors and environmental implications.
621 Appl. Geochem 17, 961–973.
622 Navas, A., Lindhorfer, H., 2003. Geochemical speciation of heavy metals in
623 semiarid soils of the central Ebro Valley (Spain). Environment International 29(1), 61–
624 68.
625 Navas, A., Soto, J., Machín, J., 2005. Mobility of natural radionuclides and selected
626 major and trace elements along a soil toposequence in the central Spanish Pyrenees.
627 Soil Sci. 170 (9), 743–757.
628 Navas, A., Machín, J., Beguería, S., López-Vicente, M., Gaspar, L., 2008. Soil
629 properties and physiographic factors controlling the natural vegetation re-growth in a
630 disturbed catchment of the Central Spanish Pyrenees. Agroforestry Syst 72, 173-185.

631 Navas, A., López-Vicente, M., Gaspar, L., Machín, J., 2013. Assessing soil
632 redistribution in a complex karst catchment using fallout ^{137}Cs and GIS.
633 Geomorphology 196, 231–241.
634 Oldfield, F., Wu, R., 2000. The magnetic properties of the recent sediments of
635 Brothers Water, N W England. J. Paleolimnol. 2 (2):165–174.
636 Owens, P.N.,Walling, D.E., 2002. The phosphorus content of fluvial sediment in
637 rural and industrialized river basins. Water Res. 36, 685–701.
638 Owens, P.N., Blake, W.H., Gaspar, L., Gateuille, D., Koiter, A.J., Lobb, D.A.,
639 Petticrew, E.L., Raiffarth, D., Smith, H.G., Woodward, J.C., 2016. Fingerprinting and
640 tracing the sources of soils and sediments: earth and ocean science, geoarchaeological,
641 forensic, and human health applications. Earth Sci. Rev. 162, 1–23.
642 Palazón, L., Latorre B., Gaspar, L., Blake, W.H., Smith, H.G., Navas, A., 2015.
643 Comparing catchment sediment fingerprinting procedures using an auto-evaluation
644 approach with virtual sample mixtures. Science of the Total Environment 532, 456–466.
645 Palmer, J.A., Schilling, K.E., Isenhart, T.M., Schultz, R.C., Tomer, M.D., 2014.
646 Streambank erosion rates and loads within a single watershed: bridging the gap between
647 temporal and spatial scales. Geomorphology 209, 66–78.
648 Pulley, S., Rowntree, K., 2016. The use of an ordinary colour scanner to fingerprint
649 sediment sources in the South African Karoo. J. Environ. Manage 165, 253–262.
650 Quijano, L., Chaparro, M.A.E., Marié, D.C., Gaspar, L., Navas, A., 2014. Relevant
651 magnetic and soil parameters as potential indicators of soil conservation status of
652 Mediterranean agroecosystems. Geophys. J. Int. 198, 1805–1817.
653 Quijano, L., Gaspar, L., Navas, A. 2016. Spatial patterns of SOC, SON, ^{137}Cs and
654 soil properties as affected by redistribution processes in a Mediterranean cultivated field
655 (Central Ebro Basin). Soil & Tillage Research 155, 318–328.

Revel-Rolland, M., Arnaud, F., Chapron, E., Desmet, M., Givelet, N., Alibert, C., McCulloch, M., 2005. Sr and Nd isotopes as tracers of clastic sources in Lake Le Bourget sediment (NW Alps, France) during the Little Ice Age: palaeohydrology implications. Chem. Geol. 224, 183–200.

Rowntree, K.M., van der Waal, B.W., Pulley, S., 2017. Magnetic susceptibility as a simple tracer for fluvial sediment source ascription during storm events. J. Environ. Manag. 194, 54–62.

Smith, H.G., Karam, D.S., Lennard, A.T., 2018. Evaluating tracer selection for catchment sediment fingerprinting. Journal of Soil and Sediments 18, 3005–3019.

Vidal, M., 1988. Contenido y dinámica del fósforo en el sedimento de praderas de fanerógamas marinas. Oecologia aquatica, 9: 41-59.

Wallbrink, P.J., Murray, A.S., Olley, J.M., Olive, L.J., 1998. Determining sources andtransit times of suspended sediment in the Murrumbidgee River, New South Wales, Australia, using fallout ^{137}Cs and ^{210}Pb. Water Resour. Res. 34, 879–887.

Walling, D.E., 2005. Tracing suspended sediment sources in catchments and river systems. Science of the Total Environment 344, 159–184.

Walling, D.E., 2013. The evolution of sediment source fingerprinting investigations in fluvial systems. J. Soils Sediments 1310, 1658e–1675.

Walling, D.E., Webb, B.W., 1982. Sediment availability and the prediction of storm-period sediment yields.Recent Developments in the Explanation and Prediction of Erosion and Sediment Yield, IAHS Publication, vol. 137, 327–337.

Walling, D.E., Collins, A.L., Stroud, R.W. 2008. Tracing Suspended Sediment and Particulate Phosphorus Sources in Catchments. *Journal of Hydrology* 350, 274-289.

Withers, P.J.A., Jarvie, H.P., 2008. Delivery and cycling of phosphorus in rivers: a review. Sci. Total Environ. 400, 379–395.

Withers, P.J.A., Jarvie, H.P., 2008. Delivery and cycling of phosphorus in rivers: a review. Sci. Total Environ. 400, 379–395.

Wynn, T., 2006, Streambank retreat-A primer: Watershed Update, January–March 2006, American Water Resources Association Hydrology and Watershed Management Technical Committee, v. 4, no. 1, p. 1–14, accessed February 15, 2014.

686 **Figures**

687

688 **Figure 1** *Vandunchil* and *La Reina* catchments: the orto-picture of the study area, the
689 location of sediment sources and sediment mixtures samples, and the different sampling
690 devices.

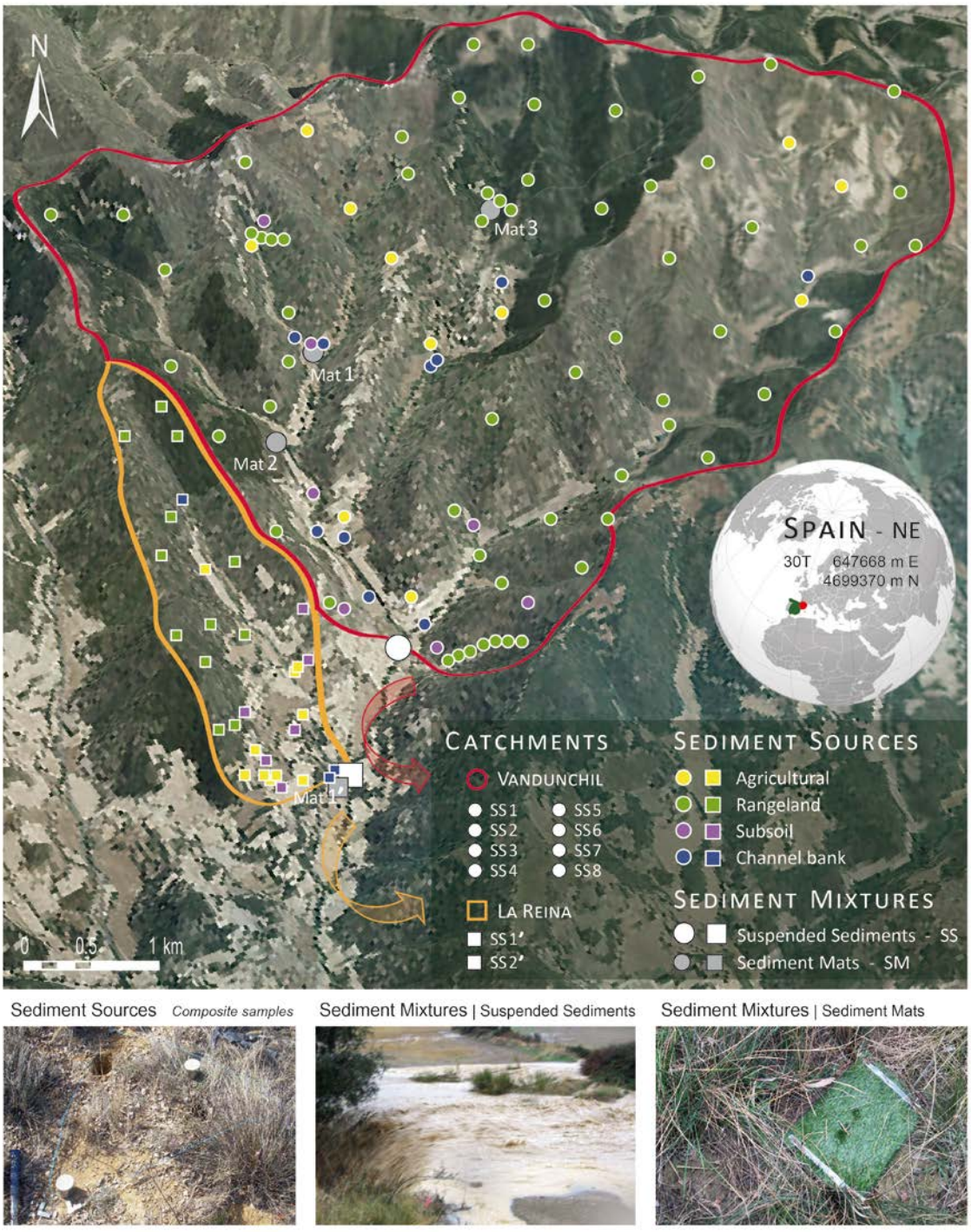

691

692 **Figure 2** Historical intraday data for the exceptional rainfall event: a) rainfall depth for
693 Yesa WS and Novellacos site, b) 15 minutes hydrograph for Yesa WS, and c) detailed
694 information for the temporal dynamic of the precipitation: peak intensity and the
695 cumulative rainfall during the collection of suspended sediments on October 19, 2012.
696

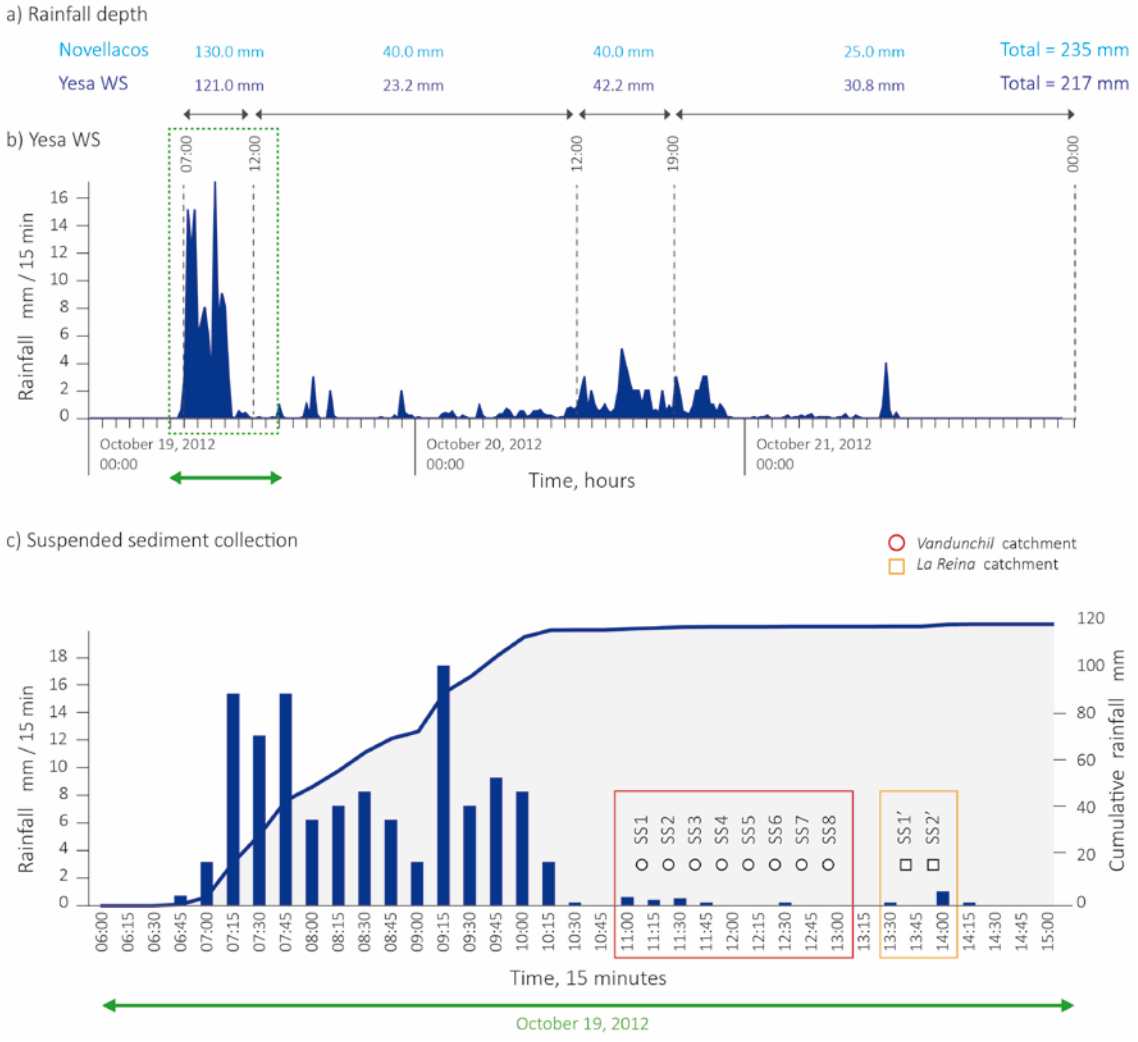

697

698 **Figure 3** Photos showing the impacts on the study area during and after the exceptional
699 rainfall event.

700

701

702

703 **Figure 4** The variation of the content on 27 properties in the time-integrated sequence
704 of eight suspended sediments samples collected at *Vandunchil* catchment.

705

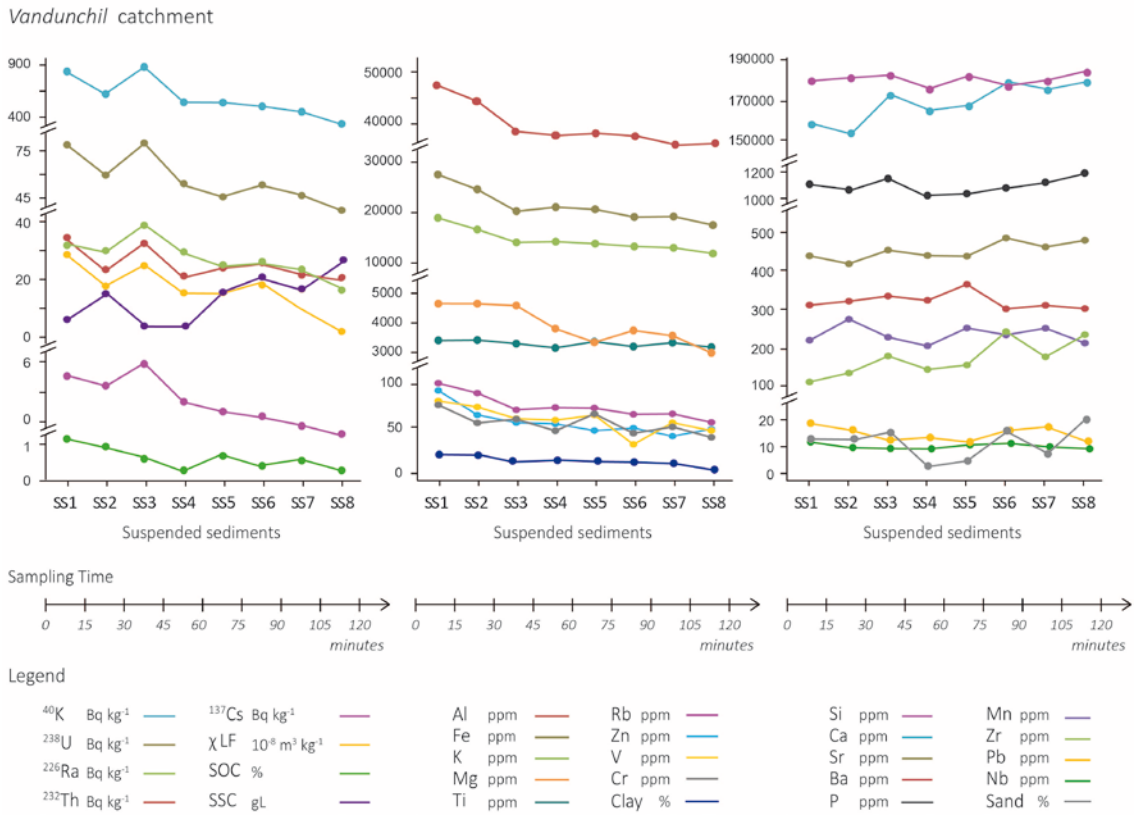

706

707

708 **Figure 5** Two-dimensional scatterplots of the first and second discriminant functions
709 from stepwise discriminant function analysis (DFA) using the optimum tracer selected
710 for a) *Vandunchil* catchment and b) *La Reina* catchment. Ellipsoid encompasses 95% of
711 group range

712

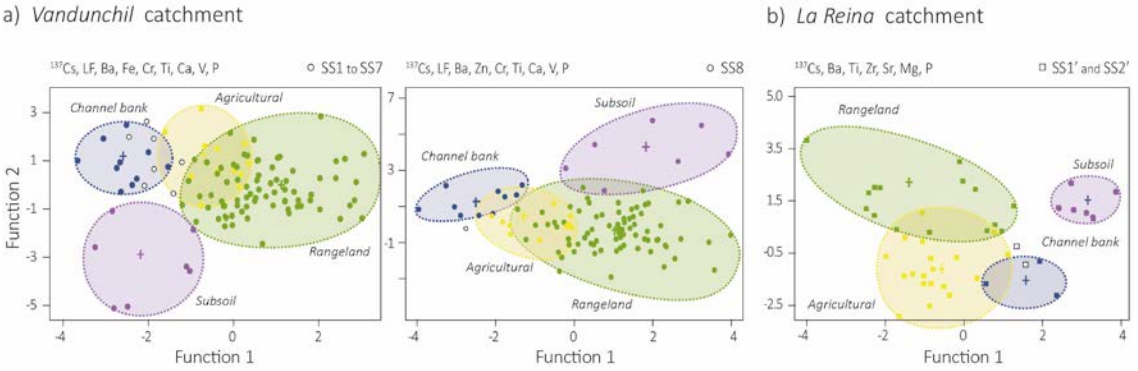

713

714

715 **Figure 6** Estimated source contribution and frequency distribution for the sediments
716 mixtures collected at *Vandunchil* catchment: a) for the time-integrated sequence of eight
717 suspended sediments (SS1 to SS8) and b) for sediment entrapped in mats (SM1, SM2).
718

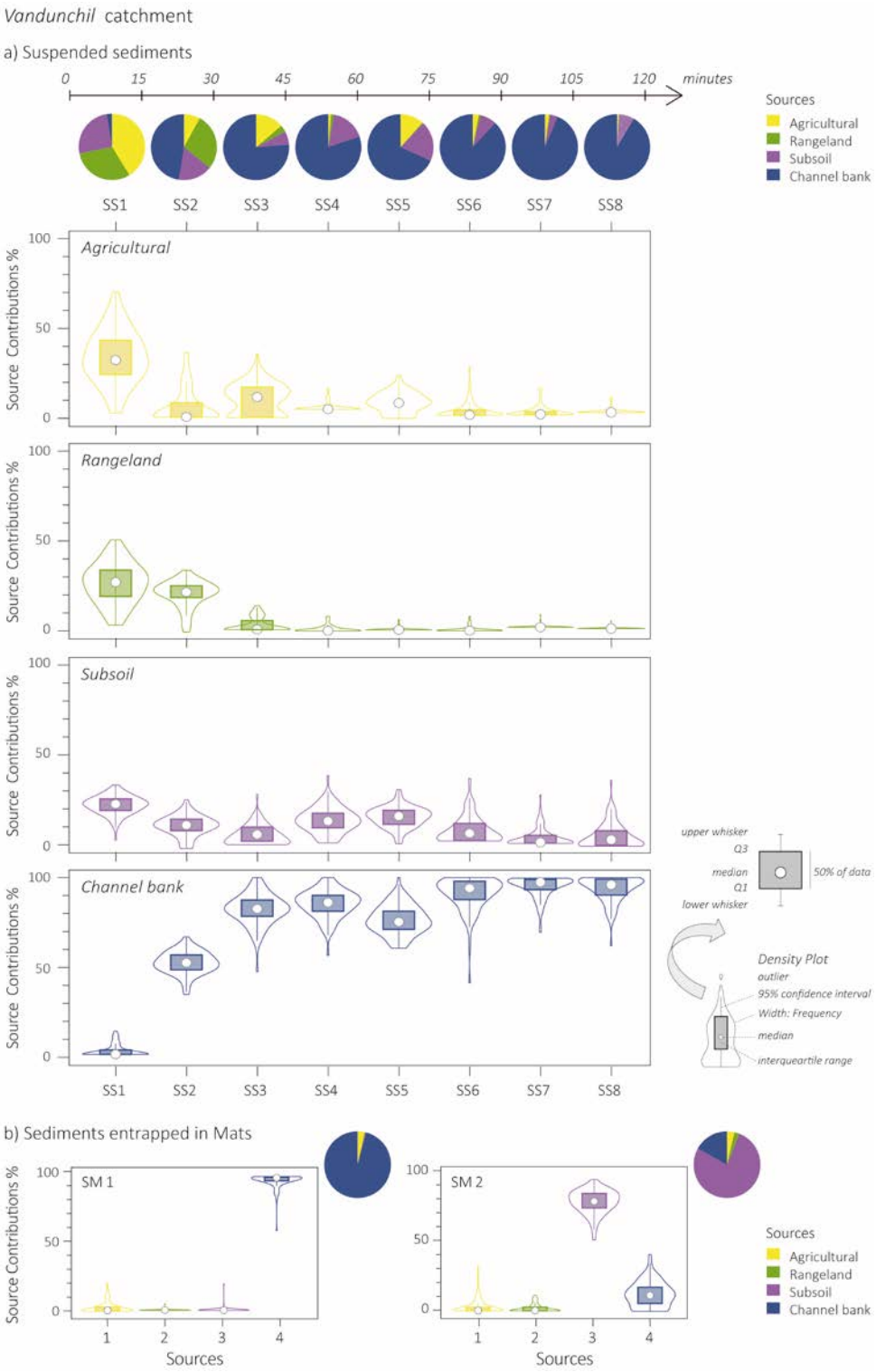

719

720 **Figure 7** Estimated source contribution and frequency distribution for the sediments
721 mixtures collected at *La Reina* catchment: a) for two suspended sediments (SS1' and
722 SS2') and b) for sediment entrapped in mats (SM1').

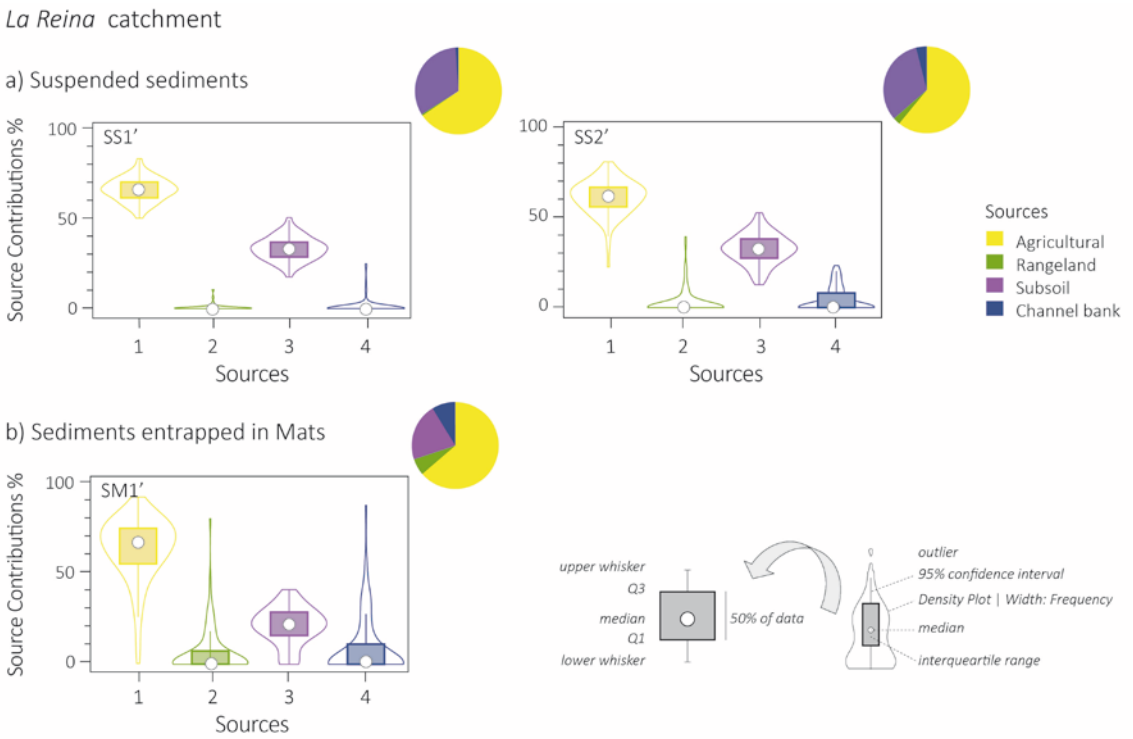

723

724

725 Table 1a. Mean content and standard deviation (SD) of all study properties for each source type
726 at the Vandunchil and La Reina catchment, respectively. Properties with significance levels for
727 discriminating between source types are shown with asterisks as potential tracers ($p < 0.05$
728 level, 95% confidence level).
729
730

		Vandunchil catchment							
		Agricultural		Rangeland		Subsoil		Channel bank	
		Mean	SD	Mean	SD	Mean	SD	Mean	SD
Si ppm	*	184672.1	13889.7	187297.2	24163.9	164464.2	5758.8	184900.7	13686.9
Ca ppm	*	148814.0	27746.6	128808.9	42756.0	171526.3	12313.3	150588.0	18706.6
Al ppm		41972.8	4064.5	40512.3	4775.4	43826.8	6261.8	39392.1	2330.4
Fe ppm	*	23997.6	2944.7	24956.8	3971.0	23611.5	3157.1	21411.6	1264.2
K ppm	*	15206.3	1484.0	15061.2	1704.2	16915.2	3469.0	14243.0	1141.6
Ti ppm	*	3451.8	324.1	3400.1	387.9	3014.4	155.9	3385.2	192.1
Mg ppm	*	4043.5	387.6	3722.9	803.6	5053.4	1524.4	3723.1	574.4
P ppm	*	1148.4	81.6	1038.4	182.7	752.4	73.2	1112.2	98.3
Ba ppm	*	313.7	38.0	279.3	38.8	370.9	64.0	340.6	29.7
Mn ppm	*	332.3	65.3	351.7	102.0	228.3	21.5	294.3	73.7
Sr ppm	*	351.8	73.6	317.9	130.2	545.5	187.3	422.7	81.1
Zr ppm	*	209.6	30.9	222.9	58.6	142.1	47.6	227.8	52.9
Rb ppm	*	79.5	10.5	79.3	11.4	88.8	19.8	72.5	6.3
Cr ppm	*	79.9	11.4	80.3	12.7	70.4	11.8	59.4	11.7
Zn ppm	*	61.7	9.8	61.2	8.9	59.4	12.1	52.3	4.1
V ppm	*	68.4	14.4	72.8	15.3	83.2	16.7	61.7	9.5
Nb ppm		11.6	1.3	11.3	1.6	10.7	0.6	11.1	0.7
Pb ppm	*	16.3	2.9	18.0	5.0	12.9	1.4	14.3	2.2
^{137}Cs Bq kg^{-1}	*	4.9	2.1	13.5	7.5	0.2	0.5	0.6	1.1
^{40}k Bq kg^{-1}		521.2	51.2	520.1	59.3	569.1	121.6	494.6	59.1
^{226}Ra Bq kg^{-1}		29.6	3.1	29.0	4.5	28.7	3.1	28.1	3.4
^{232}Th Bq kg^{-1}		34.0	3.6	34.9	4.9	34.1	4.1	33.6	2.7
^{238}U Bq kg^{-1}		44.3	6.4	44.0	10.3	45.0	9.6	40.9	10.0
LF 10^{-8} m^{3}kg^{-1}	*	59.8	21.7	62.4	32.8	10.7	5.4	19.7	8.7
SOC %	*	1.6	0.6	2.6	1.2	0.4	0.3	1.2	0.3
Clay %		17.0	2.4	14.9	3.6	13.9	4.2	13.9	1.7
Sand %	*	5.5	3.1	12.0	6.7	10.6	6.0	13.2	4.9

731

732

733 Table 1b. Mean content and standard deviation (SD) of all study properties for each source type
734 at the Vandunchil and La Reina catchment, respectively. Properties with significance levels for
735 discriminating between source types are shown with asterisks as potential tracers ($p < 0.05$
736 level, 95% confidence level).
737
738

		La Reina catchment							
		Agricultural		Rangeland		Subsoil		Channel bank	
		Mean	SD	Mean	SD	Mean	SD	Mean	SD
Si ppm		166985.4	7858.2	164725.7	17978.3	162078.6	5995.5	172081.8	2057.6
Ca ppm		170741.5	13007.6	166180.4	29243.5	177940.8	19717.6	169860.6	8957.0
Al ppm		37963.7	2965.6	35247.4	5766.2	41150.1	7312.3	37396.6	3137.7
Fe ppm		21097.1	1594.1	20699.1	3231.8	21750.8	3795.9	19566.5	2151.8
K ppm		14320.6	1186.1	13375.2	2054.7	15249.9	3458.0	13288.8	1482.5
Ti ppm	*	3142.0	171.6	3059.9	234.4	2851.3	191.4	3168.7	97.4
Mg ppm	*	3407.2	728.7	3153.5	1049.1	5219.2	1447.2	4382.4	920.4
P ppm	*	1105.7	110.3	965.5	217.9	748.2	53.5	990.6	38.8
Ba ppm	*	283.9	43.2	285.8	31.5	353.0	25.6	333.9	33.1
Mn ppm		286.8	57.7	279.9	69.6	297.2	51.2	270.2	83.0
Sr ppm	*	455.9	49.2	434.1	180.2	622.6	151.6	583.7	60.1
Zr ppm	*	186.8	26.9	215.3	48.6	161.8	51.0	236.7	11.4
Rb ppm		72.1	7.5	67.7	12.7	78.2	20.1	66.3	8.7
Cr ppm	*	69.7	7.9	69.7	12.6	65.4	12.8	51.5	9.7
Zn ppm		54.8	5.0	52.9	8.6	55.0	13.0	51.4	2.8
V ppm		58.1	9.9	60.6	12.8	72.7	19.4	57.0	15.7
Nb ppm		10.6	0.7	10.2	1.5	10.0	0.7	10.2	1.2
Pb ppm		14.9	2.1	15.4	3.8	13.7	3.4	13.7	2.4
^{137}Cs Bq kg^{-1}	*	2.6	1.3	9.2	7.2	0.2	0.5	0.4	0.7
^{40}k Bq kg^{-1}		461.2	46.0	464.4	68.6	522.3	128.1	466.7	56.8
^{226}Ra Bq kg^{-1}	*	30.5	2.3	27.8	3.1	27.5	0.7	27.8	0.6
^{232}Th Bq kg^{-1}		30.8	2.5	31.4	3.3	31.8	5.3	31.7	3.2
^{238}U Bq kg^{-1}		36.5	10.0	37.8	4.6	38.5	4.5	35.3	3.1
LF 10^{-8} m^{3}kg^{-1}	*	36.3	17.0	37.5	26.2	10.9	2.5	17.8	15.4
SOC %	*	1.0	0.2	2.1	1.0	0.3	0.2	1.1	0.2
Clay %		12.6	2.5	13.3	2.7	11.7	3.7	10.7	2.9
Sand %	*	8.2	1.9	11.2	5.3	16.5	9.7	17.1	2.0

739
740

741 Table 2. Optimum fingerprint tracers obtained with the assessed statistical
742 test (range test, Kruskal Wallis test and DFA test) for each of suspended
743 sediments (SS) and sediment mats (SM) collected at the two study
744 catchments.
745
746

Sediment mixtures	n	Tracers
Vandunchil catchment		
SS 1, SS 2, SS 3, SS 4, SS 5, SS 6, SS 7	9	^{137}Cs, LF, Ba, Fe, Cr, Ti, Ca, V, P
SS 8	9	^{137}Cs, LF, Ba, Zn, Cr, Ti, Ca, V, P
SM 1	7	^{137}Cs, LF, Ba, Cr, Ti, Ca, V
SM 2	6	^{137}Cs, LF, Ca, V, Sr, P
SM 3	6	^{137}Cs, LF, Ba, Cr, Zr, P
La Reina catchment		
SS 1', SS 2'	7	^{137}Cs, Ba, Ti, Zr, Sr, Mg, P
SM 1'	5	^{137}Cs, Ba, Ti, Mg, P

747
748

749 Table 3. Source contributions (%) estimated with FingerPro unmixing model
750 for the eight suspended sediments (SS) and the sediment mats (SM)
751 collected at the *Vandunchil* catchment. Three different simulations for each
752 sediment mixture are listed: i) using the optimum tracers, ii) excluding P as
753 a tracer, or iii) adding SOM as an additional tracer.
754

Vandunchil Sediment mixtures		GOF	Agricultural		Rangeland		Subsoil		Chanel bank	
		%	mean	SD	mean	SD	mean	SD	mean	SD
SS 1	i	78.7	41.2	19.4	30.6	14.9	25.7	6.8	2.5	4.4
	ii	74.8	22.0	18.6	33.3	14.3	44.4	8.7	0.2	1.2
	iii	79.1	39.8	19.9	0.2	1.2	28.6	6.9	4.0	5.8
SS 2	i	81.7	8.0	12.2	27.7	9.8	16.8	7.5	47.5	8.2
	ii	74.3	10.2	14.9	23.1	11.2	39.1	10.3	27.6	11.2
	iii	81.7	8.4	13.0	24.1	9.2	19.8	7.4	47.7	9.3
SS 3	i	76.7	13.8	11.3	3.4	5.2	6.6	6.6	76.2	11.3
	ii	72.9	10.3	10.4	2.9	4.6	24.6	10.2	62.2	12.7
	iii	77.4	11.3	9.6	1.9	3.4	7.8	5.7	79.0	10.7
SS 4	i	75.4	1.3	3.2	1.4	2.5	17.1	9.2	80.2	10.0
	ii	67.8	2.3	5.3	0.8	1.9	36.3	13.5	60.6	14.0
	iii	76.0	1.2	4.1	0.4	1.0	18.3	7.7	80.1	9.6
SS 5	i	84.8	11.6	7.4	0.4	1.3	19.7	7.5	68.2	10.6
	ii	78.1	10.4	9.7	0.3	1.2	38.3	9.7	51.0	13.2
	iii	86.0	9.7	7.1	0.1	0.8	20.7	6.1	69.4	9.7
SS 6	i	64.0	3.0	5.8	0.8	2.1	8.2	9.8	88.0	12.2
	ii	63.2	1.6	4.1	0.9	2.2	4.9	7.7	92.6	9.1
	iii	65.8	2.2	5.8	0.2	0.2	7.7	8.4	89.9	12.0
SS 7	i	75.6	2.1	4.1	0.3	1.1	3.9	6.3	93.6	7.7
	ii	70.2	2.6	5.4	0.2	0.6	20.5	12.0	76.8	13.0
	iii	76.8	1.5	3.4	0.1	0.2	3.6	5.1	94.8	6.5
SS 8	i	67.3	0.7	2.0	0.3	0.7	7.5	9.1	91.5	9.3
	ii	69.5	0.6	2.3	0.2	0.3	11.6	9.7	87.6	10.3
	iii	68.9	0.8	2.6	0.1	0.1	6.9	7.9	92.2	8.8
SM 1	i	68.1	3.4	5.6	0.3	0.7	0.5	2.7	95.7	7.1
	ii	68.1	3.4	5.6	0.3	0.7	0.5	2.7	95.7	7.1
	iii	67.2	2.4	6.0	0.2	0.2	1.9	5.5	95.5	9.1
SM 2	i	80.6	3.6	7.4	2.4	4.0	77.1	11.7	16.9	12.8
	ii	79.3	0.8	2.8	3.1	4.1	82.3	18.5	13.8	19.0
	iii	90.1	0.7	3.2	4.2	4.4	54.8	9.8	40.3	12.4
SM 3	i	-	-	-	-	-	-	-	-	-
	ii	-	-	-	-	-	-	-	-	-
	iii	-	-	-	-	-	-	-	-	-

755 Table 4. Source contributions (%) estimated with FingerPro unmixing model
756 for the two suspended sediments (SS) and the sediment mat (SM) collected
757 at the *La Reina* catchment. Three different simulations for each sediment
758 mixture are listed: i) using the optimum tracers, ii) excluding P as a tracer,
759 or iii) adding SOM as an additional tracer.
760
761

La Reina Sediment mixtures		GOF	Agricultural		Rangeland		Subsoil		Chanel bank	
		%	mean	SD	mean	SD	mean	SD	mean	SD
SS 1’	i	83.6	65.4	6.5	0.6	1.7	32.9	6.4	1.1	3.9
	ii	81.3	66.8	10.0	0.7	2.9	31.0	7.2	1.5	5.3
	iii	83.2	65.5	6.7	0.2	0.7	32.8	6.5	1.5	4.0
SS 2’	i	78.1	60.9	9.6	2.7	6.8	32.4	8.2	4.0	6.5
	ii	78.4	64.3	14.8	1.8	7.6	29.8	9.4	4.1	9.1
	iii	78.1	60.9	9.6	2.7	6.8	32.4	8.2	4.0	6.5
SM 1’	i	76.6	63.7	17.4	6.2	12.2	21.4	10.3	8.7	15.8
	ii	72.5	59.2	21.4	10.7	17.1	24.3	12.3	5.7	14.4
	iii	69.2	50.1	19.5	1.2	3.6	30.1	11.6	18.5	25.3

762
763
764